

## ANTI-XANTHINE OXIDASE ACTIVITY OF FLAVONE ANALOGUES FROM *Dillenia indica* L. AND *IN SILICO* STUDY

T. Khammee<sup>1,\*</sup>, A. Rattanapittayaporn<sup>2</sup>, C. Rangjaroen<sup>3</sup>,  
A. Jaratrungtawe<sup>4</sup> and M. Kuno<sup>5</sup>

<sup>1</sup>Department of Chemistry, Faculty of Science and Technology, Phranakhon Rajabhat University, Bangkok, Bangkok, 10220, Thailand

<sup>2</sup>Department of Cosmetic Science, Faculty of Science and Technology, Phranakhon Rajabhat University, Bangkok, Bangkok, 10220, Thailand

<sup>3</sup>Department of Agricultural Technology, Faculty of Science and Technology, Phranakhon Rajabhat University, Bangkok, Bangkok, 10220, Thailand

<sup>4</sup>Bruker Biospin AG, Sathorn, Bangkok, 10120, Thailand

<sup>5</sup>Department of Chemistry, Faculty of Science, Srinakharinwirot University, Prasarnmit 23, Watthana, Bangkok, 10110, Thailand

\*E-mail: [thongchai.k@pnru.ac.th](mailto:thongchai.k@pnru.ac.th)

### ABSTRACT

Six bioactive substances have been isolated from the fruit extract of *Dillenia indica* L., including a triterpene lupeol (**1**), together with a mixture of  $\beta$ -sitosterol (**2a**) and stigmasterol (**2b**), three flavonols, keamferide (**3**), dillenetin (**4**), quercetin (**5**), and  $\beta$ -sitosterol-d-glucoside (**6**). The structures of all isolated compounds were characterized by analysis of their spectroscopic data and by comparison with the reported value of the known compounds. The investigation of anti-xanthine oxidase activity shows that compounds **3**, **4**, and **5** were suitable xanthine oxidase inhibitors, with IC<sub>50</sub> value in the range of 0.56-1.44 mM. Moreover, a molecular docking study of a potent xanthine oxidase inhibitor was performed to find the binding mode of the inhibitors into the binding site of xanthine oxidase.

**Keywords:** Anti-xanthine Oxidase, Flavone, *Dillenia indica* L., Molecular Docking.

© RASĀYAN. All rights reserved

### INTRODUCTION

Gout is an inflammatory, metabolic joint disease and characterized by the formation of monosodium urate crystals that accumulate in the synovial joints and other tissues. The prevalence of gout and hyperuricemia has been reported to be increasing worldwide.<sup>1,2</sup> Therefore, the use of xanthine oxidase inhibitors that block uric acid production is one of the therapeutic approaches to the treatment of gout.

Xanthine oxidase (XO) is a fascinating target for rational drug design and mechanism-based inhibitors development because it plays a role in catalyzing hypoxanthine to xanthine metabolism and xanthine to uric acid approaches. XO inhibitors blocking the concluding step in uric acid biosynthesis can reduce the level of the plasma uric acid concentration and also are commonly applied for the treatment of gout.<sup>3</sup> Among commercially available XO inhibitors, allopurinol is the most effective approach to treat gouty arthritis. However, allopurinol is known to have limitations for clinical use due to their unfavorable side-effects, including hypersensitivity reaction, renal toxicity, Steven-Johnson syndrome, and epidermal necrolysis.<sup>4,5</sup> Consequently, the exploration for novel XO inhibitors with extra outstanding biological activity and fewer adverse side effects is aspired not only to manage gout but also to resist several other diseases correlated with the XO activity. The usage of biological substances is receiving recommended interest as the possible source of new drugs in the exploration of new medications for the treatment of various diseases.<sup>6</sup> Natural products adapted from conventional therapeutic plants have continually

proffered an attractive probability for the evolution of novel medicinal agents.<sup>7-9</sup> Natural products provide high XO inhibitors that can be improved toward clinical products.<sup>10</sup> At present, the potential for the development of successful natural products for the managing of XO-linked diseases is still practically unknown. Continuing with the study of the medicinal plant from Thailand as a source of new secondary metabolites with a diverse grade of biological activities and the fact that there still is an excellent interested in finding novel and better XO inhibitors, which prompted us to screen the fruit of *Dillenia indica* L. (Dilleniaceae) for their XO inhibitory activities. *D. indica* (elephant apple) or Matad is a common evergreen tree that grows widely in tropical forests and uses as an integral part of the local recipe, which has more to it than just its taste and flavor.<sup>11</sup> The pharmacological activity was evaluated and showed that the leaves, bark, fruits or the various part of the *D. Indica* have high medicinal values. It possesses various activities like antimicrobial, antioxidant, analgesic, anti-inflammatory, dysentery, antidiabetic and central nervous system (CNS) depressant activity.<sup>12-15</sup> In the present investigation, an endeavor was made to concentrate on the effectiveness of *D. indica* as anti-gout. The chemical constituents of *D. indica* were evaluated for their potential XO inhibitory activity. Subsequently, the *in silico* molecular docking study was launched to investigate the molecular interactions amid the active structures and target enzymes.

## EXPERIMENTAL

### General Procedure

UV spectra were measured on a Perkin Elmer VICTOR Nivo. Attenuated total reflection infrared (ATR-FTIR) spectra were obtained on a Bruker TENSOR II FTIR spectrophotometer.

<sup>1</sup>H- and <sup>13</sup>C-NMR spectra were obtained on a Bruker AVANCE 300 FT-NMR spectrometer and a Bruker AVANCE III 500 NMR spectrometer, determined at 300 MHz and 500 MHz (<sup>1</sup>H) and 75 MHz (<sup>13</sup>C). For the spectra recorded in chloroform-d, acetone-d<sub>6</sub> and dimethyl sulfoxide-d<sub>6</sub>, the signals of non-deuterated residual at  $\delta_H$  7.24,  $\delta_H$  2.04 and  $\delta_H$  2.50 ppm and the solvent signals at  $\delta_C$  77.00,  $\delta_C$  29.80 and  $\delta_C$  39.5 ppm were applied as references for <sup>1</sup>H- and <sup>13</sup>C-NMR spectra, respectively. Column chromatography (CC) was carried out using Merck silica gel 60 (0.040-0.063 mm, cat. No. 109385, and (<0.063 mm, cat. No. 107729). Thin-layer chromatography (TLC) was done on precoated Merck silica gel 60 F<sub>254</sub> (cat. No. 105554) plates, thickness 2.00 mm. The spots on developed TLC were visualized under visible light, UV light (wavelength 254 nm and 365 nm), and by spraying with a solution of *p*-anisaldehyde-H<sub>2</sub>SO<sub>4</sub> reagent followed by heating at 100°C until spots appear. Melting point measurements have been done on a Griffin melting point apparatus in degree Celsius of temperature. XO (EC 1.2.3.2) from bovine milk ( $\geq 0.4$  units/mg) and xanthine were obtained from Sigma-Aldrich Co. LLC (MO, USA). Allopurinol was purchased from Sigma-Aldrich Co. LLC (MO, USA). All other reagents were of the highest grade available commercially.

### Plant Material

The fruits of *D. indica* were collected from Pakkred, Nonthaburi, Thailand (13.906289, 100.483087), in September, 2017. The plant was identified by comparison with the herbarium at Forest Herbarium, Department of National Park, Wildlife and Plant Conservation, Ministry of Natural Resources and Environment, Bangkok. A voucher specimen (PNRU 2017001) was deposited at the Department of Chemistry, Faculty of Science and Technology, Phranakhon Rajabhat University, Bangkok, Thailand.

### Extraction and Isolation

The fresh fruits of *D. indica* were cleaned and cut into smaller pieces. The total amount of *D. indica* was 3.5 kg. The fruits were exhaustively extracted three times with acetone, each time for a week. The combined acetone extract was evaporated in vacuo by using the Büchi rotary evaporator at 45°C gave the resulting as dark brown residue (213.4 g, 6.1%).

The 41.4 g of acetone crude extract was fractionated by quick column chromatography (QCC) on silica gel column (silica gel 60 cat. No. 109385, 150 g) using a gradient of *n*-hexane-acetone (0-100%, stepwise). The fractions had been collected and checked via TLC on silica gel PF<sub>254</sub>. Fractions with spots displaying comparable profiles were mixed and gave 10 broad fractions. Fraction 2 (353.9 mg) was

subjected to column chromatography (silica gel 60 cat. No. 7729) employing a gradient of *n*-hexane and acetone, which resulted in 9 subfractions. Subfraction 2.2 was proved to be a compound **1** (39.7 mg, lupeol, 0.09%). In addition, subfraction 2.5 was found to be a mixture of **2** (30.1 mg,  $\beta$ -sitosterol and stigmasterol, 0.07%). Fraction 3 (2.67 g) becomes purified through CC on silica gel (cat. No. 109385) and eluted with a gradient of *n*-hexane-acetone to give 7 subfractions. Subfraction 3.4 was further filtered and rinsed with cool hexane AR grade to provide a yellow solid of **3** (1.05 g, kaempferide, 2.53%). Fraction 4 (475.3 mg) was also isolated by CC over silica gel (cat. No. 109385), applying a gradient of acetone-*n*-hexane to afford seven subfractions. The purification of subfraction 4.4 (209.8 mg) was performed by CC over silica gel (cat. No. 107729) to give compound **4** (dillenetin), which was recrystallized from  $\text{CH}_2\text{Cl}_2$ -MeOH (10-90) to obtain as yellow needles (55.7 mg, dillenetin, 0.13%). The isolation process of fraction 6 (2.13 g) was accomplished by a silica gel (cat. No. 109385) column eluted with the gradient system of *n*-hexane-acetone to give nine subfractions. The subfractions 6.5 was purified by recrystallization using  $\text{CH}_2\text{Cl}_2$ -MeOH (90-10) as a solvent to obtain as yellow needles compounds **5** (935.7 mg, quercetin, 2.66%). The fraction 9 (1.93 g) was separated by the CC method on silica gel and using a gradient of  $\text{CH}_2\text{Cl}_2$ -MeOH as the mobile phase to give 7 subfractions. Compound **6** was obtained as white solid by washing the subfraction 9.5 with cold dichloromethane (23.2 mg,  $\beta$ -sitosterol-d-glucoside, 0.05%).

### Lupeol (1)

White solid; mp. 203-205°C [lit. mp. 213.8-215.2°C<sup>16</sup>];  $R_f$  0.75 (5% EtOAc- $\text{CH}_2\text{Cl}_2$ ); ATR-FTIR  $\text{cm}^{-1}$ : 3304, 1457, 1378, 1038;  $^1\text{H-NMR}$  ( $\text{CDCl}_3$  300 MHz)  $\delta$ : 4.66 (1H, br s, H-29a), 4.54 (1H, br s, H-29a), 3.16 (1H, dd,  $J = 10.8, 5.2$  Hz, H-3), 2.35 (1H, ddd,  $J = 11.0, 11.0, 5.5$  Hz, H-19), 1.00 (3H, s, H-26), 1.65 (3H, s, H-30), 0.94 (3H, s, H-23), 0.80 (3H, s, H-25), 0.76 (3H, s, H-24), 0.73 (3H, s, H-28), 0.65 (1H, d,  $J = 8.8$  Hz, H-5), identical to the literature data<sup>17,18</sup>; HR-APCI-TOFMS: (+ve):  $m/z$  427.3984 (calcd. for  $\text{C}_{30}\text{H}_{50}\text{O}+\text{H}$ : 427.3934).

### A mixture $\beta$ -sitosterol and stigmasterol (2)

White solid; mp. 151-153°C [lit. mp. 145-147°C °C<sup>19</sup>];  $R_f$  0.42 (5% EtOAc- $\text{CH}_2\text{Cl}_2$ ); ATR-FTIR  $\text{cm}^{-1}$ : 3371, 2916, 1732, 1462, 1068, 1021;  $^1\text{H-NMR}$  ( $\text{CDCl}_3$  300 MHz)  $\delta$ : 5.32 (2H, br d,  $J = 4.3$  Hz, H-6), 5.13 (1H, dd,  $J = 15.1, 8.4$  Hz, H-23), 4.96 (1H, dd,  $J = 15.1, 8.4$  Hz, H-22), 3.49 (2H, m, H-3), 1.00 (6H, s, H-19), 0.98 (6H,  $J = 6.6$  Hz, H-21), 0.85 (6H, d,  $J = 3.3$  Hz, H-29), 0.84 (6H, d,  $J = 6.4$  Hz, H-26), 0.82 (6H, d,  $J = 6.4$  Hz, H-27), 0.77 (6H, s, H-18), identical to the literature data<sup>20</sup>; HR-APCI-TOFMS: (+ve):  $m/z$  415.3951 (calcd. for  $\text{C}_{29}\text{H}_{50}\text{O}+\text{H}$ : 415.3934).

### Kaempferide (3)

Yellow solid; mp. 226°-228°C [lit. mp. 224°-226°C<sup>21</sup>];  $R_f$  0.5 (40% acetone-hexane);  $\lambda_{\text{max}}^{\text{MeOH}}$  nm (log  $\epsilon$ ): 247 (3.02), 260 (3.00), 298 (2.99), 362 (2.93), 395 (2.91); ATR-FTIR  $\text{cm}^{-1}$ : 3463, 1651, 1614, 1293, 1170;  $^1\text{H}$ - and  $^{13}\text{C}$ -NMR data, see Table-1; HR-ESI-TOFMS: (+ve):  $m/z$  301.0712 (calcd. for  $\text{C}_{16}\text{H}_{12}\text{O}_6+\text{H}$ : 301.0706).

### Dillenetin (4)

Yellow needles; mp. 292-294 °C [lit. mp. 291-292°C<sup>22</sup>];  $R_f$  0.42 (30% acetone-hexane);  $\lambda_{\text{max}}^{\text{MeOH}}$  nm (log  $\epsilon$ ): 249 (3.12), 299 (3.11), 359 (3.06), 393 (3.06); ATR-FTIR  $\text{cm}^{-1}$ : 3430, 3280, 1649, 1596 1251, 1144;  $^1\text{H}$ - and  $^{13}\text{C}$ -NMR data, see Table-1; HR-ESI-TOFMS: (+ve):  $m/z$  331.0812 (calcd. for  $\text{C}_{17}\text{H}_{14}\text{O}_7+\text{H}$ : 331.0812).

### Quercetin (5)

Yellow needles; mp. 310-312°C [lit. mp. 313-314°C<sup>22</sup>];  $R_f$  0.25 (40% acetone-hexane);  $\lambda_{\text{max}}^{\text{MeOH}}$  nm (log  $\epsilon$ ): 247 (3.08), 260 (3.08), 297 (3.07), 359 (3.03), 394 (3.02); ATR-FTIR  $\text{cm}^{-1}$ : 3381, 1660, 1600 1194, 2275

1162;  $^1\text{H}$ - and  $^{13}\text{C}$ -NMR data, see Table-1; HR-ESI-TOFMS: (+ve):  $m/z$  303.0503 (calcd. for  $\text{C}_{15}\text{H}_{10}\text{O}_7+\text{H}$ : 303.0499).

### **$\beta$ -Sitosterol-d-glucoside (6)**

White solid; mp 272-274°C [lit. mp 272-274°C]<sup>23</sup>;  $R_f$  0.45 (10% MeOH- $\text{CH}_2\text{Cl}_2$ ); ATR-FTIR  $\text{cm}^{-1}$ : 3360, 2956, 1461, 1366, 1051, 1021;  $^1\text{H}$ -NMR ( $\text{CDCl}_3$  400 MHz)  $\delta$ : 5.37 (1H, d, H-6), 4.42 (1H, d,  $J = 7.8$  Hz, H-1'), 3.43 (4H, m, H-2', H-3', H-4', H-5'), 3.22 (1H, m, H-3), 3.21 (1H, m, H-6'), 2.19 (2H, m, H-4, H-25), 1.85 (4H, m, H-7, H-15, H-16, H-17), 1.34 (5H, m, H-2, H-11, H-12, H-28, H-30), 1.26 (2H, m, H-8, H-9), 1.21 (2H, m, H-1, H-14), 1.19 (4H, m, H-22, H-23), 1.13 (2H, m, H-24), 0.91 (3H, s, H-19), 0.80 (6H, s, H-21, H-29) 0.76 (3H, s, H-26), 0.70 (3H, s, H-27), 0.68 (3H, s, H-18), identical to the literature data<sup>19,24</sup>; HR-ESI-TOFMS: (+ve):  $m/z$  599.4288 (calcd. for  $\text{C}_{35}\text{H}_{60}\text{O}_6+\text{Na}$ : 599.4282).

### ***In vitro* Xanthine Oxidase Inhibitory Activity**

The xanthine oxidase inhibitory activity of the isolated compounds was investigated applying the Niu's method employing negligible modification.<sup>25</sup> The bioassay mixture comprises of 10  $\mu\text{L}$  of the test compound (18.75, 37.5, 75.0, 150.0, 300.0 and 600.0  $\mu\text{g/mL}$ ), 180.0  $\mu\text{L}$  of phosphate buffer (pH 7.5) and 10  $\mu\text{L}$  of 0.06 mM xanthine solution (in phosphate buffer, pH 7.5). The enzymatic reaction was started by adding 10  $\mu\text{L}$  of 0.4 units/mL XO enzyme solution (in phosphate buffer, pH 7.5), which was provided promptly before use by diluting from a stock enzyme solution into the buffer solution. The final mixture process became incubated at 37°C for 30 min. In the final step, 10 mL of 0.5 M HCl was applied for termination of the enzyme reaction prior to the absorbance measurement. For blank assays, a blank was assembled in an identical manner but adding 0.5 M HCl before enzyme. The absorbance was read at 295 nm in the microplate reader (Victor Nivo multimode microplate reader Perkin Elmer). All enzyme tests have been conducted in triplicate. Allopurinol, known as XO inhibitory agent (TCI, Tokyo, Japan) concentration of 5-100  $\mu\text{g/mL}$  was used as the standard. The results were considered as percentage inhibition which was calculated by the use of the following equation:

$$\text{XO Inhibitory activity (\%)} = \frac{A_c - A_s}{A_c} \times 100$$

Where  $A_s$  is the absorbance value of the test substance, and  $A_c$  is the control absorbance value.

The % XO inhibition was plotted against the extract concentration, and the  $\text{IC}_{50}$  values were obtained from the graph.

### **Statistical Analysis**

For statistical analysis, the consequences of anti-XO activity had been expressed as a mean  $\pm$  SD. The  $\text{IC}_{50}$  values had been calculated the use of the Microsoft Excel program (2016).

### **Computational Studies**

The three-dimensional coordinates of the bovine XO enzyme (Protein Data Bank, PDB ID code: 1FIQ, Resolution = 2.5 Å) were acquired from the Protein Data Bank (PDB).<sup>26</sup> The obtained protein structure (1FIQ) was prepared for molecular docking by removing of salicylic acid and water molecules from its crystal structure. Besides, the preparation of protein was achieved by AutoDock Tools (ver 1.5.4) using default parameters and subsequently saved as the pdbqt file.<sup>27</sup> The structure of selected molecules was drawn by using ACD/ChemSketch Freeware from the ACD/Labs software package and then converted into 3D structures by ACD/3D Viewer Freeware (same program package).<sup>28</sup> The ligands were optimized at Hartree-Fock with basis set 3-21G level of calculation using Gaussian 03 packages, which is then converted to mol2 file format using GaussView 3.0 software.<sup>29</sup> All optimized ligands were processed to pdbqt file format by AutoDock Tools. The ligands were docked into the binding site of XO using AutoDock 4.2. AutoDock 4.2 (Linux version) was used because its algorithm allows full flexibility of small ligands. The best conformers were examined by the Lamarckian genetic algorithm (LGA). Between the molecular docking manner, the maximum of 100 conformers was studied. The population size was

fixed at 150. The maximum number of energy evaluation was applied to 2500000. The grid-box dimensions were assigned as 100, 100 and 100 Å (x, y and z). The spacing between grid points was 0.375 Å. The grid box centered was fixed at 33.836 (x), 8.227 (y) and 30.991 (z). The lowest energy cluster rendered by AutoDock for the compound was adopted for further investigation. All other parameters were controlled at their default settings. All molecular images of docking results have generated by the usage of the Discovery Studio 3.1 Client (ver. 3.1.1.11157, Accelrys Software Inc., San Diego, CA, USA). Docking method validation was achieved by redocking the primary ligand receptor on the active site. The docking validation approach was assessed from the value root-mean-square deviation (RMSD) furthermore indicated effective if a particular value of RMSD smaller than 3.5 Å.<sup>30</sup>

## RESULTS AND DISCUSSION

The chromatographic isolation of the acetone extracts of the fruit of *D. indica* yielded six compounds (compound **1-6**, Fig.-1). The structures of separated compounds were ascertained via significant NMR spectral analysis as well as by similarity of their spectral information with previously reported values.

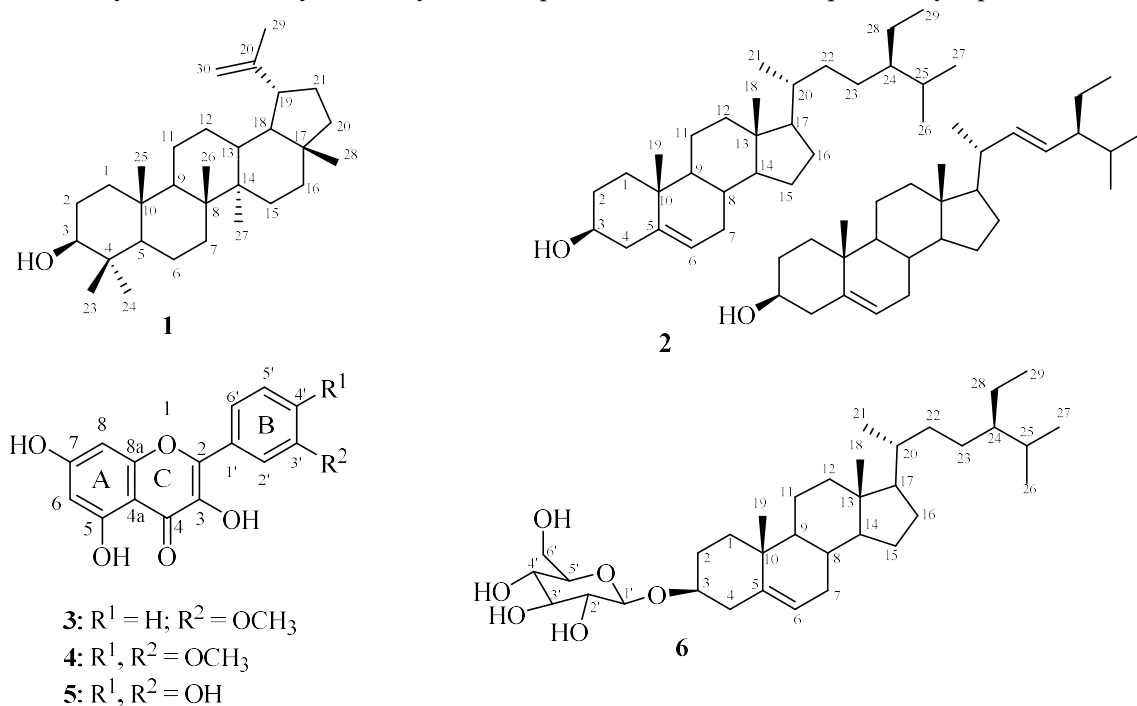


Fig.-1: Chemical Structure of Compounds **1-6**

### Structural Elucidation

Compound **1** was attained as a white amorphous solid and produced purple color with anisaldehyde-sulphuric acid on TLC. The <sup>1</sup>H-NMR spectrum of the compound **1** revealed signals of isopropenyl, which included vinylic proton at δ 4.54 (1H, br s) and 4.66 (1H, br s), and the methyl signal of isopropenyl at δ 1.65 (3H, s). The carbinol proton signal at δ 3.16 (1H, dd, *J* = 10.8, 5.2 Hz) was detected. The resonance signals of methyl groups at 0.73, 0.78, 0.80, 0.92, 0.94 and 1.00 ppm exhibited six tertiary methyl singlets. The data were in agreement with those detailed for a pentacyclic triterpenoid lupeol.<sup>18</sup> The evaluation of its physical and spectral information with published values revealed that compound **1** as lupeol (**1**).

Compound **2** was found as a white amorphous solid and detected as a purple spot by spraying anisaldehyde-sulphuric acid with the R<sub>f</sub> value of 0.42 (5% EtOAc-CH<sub>2</sub>Cl<sub>2</sub>). Its ATR-FTIR spectrum exhibited hydroxyl at 3371 cm<sup>-1</sup> and exomethylene at 1462 cm<sup>-1</sup>. The HR-APCI-TOFMS spectrum confirmed the pseudo-molecular ion (positive ion mode) at *m/z* 415.3951 corresponding to C<sub>29</sub>H<sub>50</sub>O+H. The <sup>1</sup>H-NMR displayed signal of methine olefinic proton at δ 5.32 (2H, d, *J* = 4.3 Hz), δ 5.13 (1H, dd, *J* = 15.1, 8.4 Hz) and 4.96 (1H, dd, *J* = 15.1, 8.4 Hz) and carbinol proton signal at δ 3.49 (2H, m). These data

are were entirely consistent with a mixture of  $\beta$ -sitosterol and stigmasterol (**2**). Parallelization of these data with published data proved the identification of compound **2** as a mixture of  $\beta$ -sitosterol and stigmasterol (**2**).<sup>24</sup>

NMR spectroscopic data of compounds **3**, **4**, and **5** revealed that they all showed a typical flavonol pattern consisting of two phenyl rings (A and B) and conjugated  $\gamma$ -pyrone (C) (Table-1). Compound **3** was separated as a yellow amorphous solid. The molecular formula of **3**,  $C_{16}H_{12}O_6$ , was assigned by HR-ESI-TOFMS analysis (found 301.0712 for  $C_{16}H_{12}O_6+H$ , calcd. 301.0706). UV absorption at 247, 260, 298, 362, 395 and 370 nm was indicated the significant conjugated chromophore, which suggested the presence of an aromatic moiety. The  $^1H$ -NMR spectrum data represented the characteristic peak of H-2' and H-6' as a doublet of a doublet at  $\delta$  8.22 with the coupling of 8.0 Hz whereas H-3' and H-5' with similar to ortho coupling appeared at  $\delta$  7.11 as a doublet. The  $^1H$ -NMR spectrum of compound **3** further exhibited the signals of aromatic protons as a doublet at  $\delta$  6.27 (H-6) and at  $\delta$  6.54 (H-8) showing meta coupling of 1.6 Hz. The spectrum displayed a singlet signal at  $\delta$  3.90 indicating the presence of a methoxy group. The  $^{13}C$ -NMR spectrum of compounds **3** displayed signals of nine quaternary, six methine carbons, and one methyl ether carbon. All the  $^{13}C$  assignments agreed with the reported data.<sup>18</sup> The COSY, HMQC, and HMBC correlations aided in the assignments of values of all protons for  $^1H$ -NMR and  $^{13}C$ -NMR. Compound **3** was identified as kaempferide (**3**).

Compound **4** was obtained as a yellow powder with a melting point of 292-294°C. The  $R_f$  value of compound **4** was determined as 0.42 in 30% acetone-hexane and gave an orange color with anisaldehyde-sulphuric acid on TLC. The molecular formula of compound **4** was determined to be  $C_{17}H_{14}O_7$  by HR-ESI-TOFMS molecular-ion peak at  $m/z$  331.0812 ( $[M+H]^+$ , calcd. 331.0812). The ATR-FTIR spectrum of compound **4** showed characteristic absorption bands for conjugated carbonyl at  $1649\text{ cm}^{-1}$  and hydroxyl groups at  $3430\text{ cm}^{-1}$ . The UV-Vis spectrum showed maximum absorption at wavelength 247, 260, 298, 359 and 394 nm. The  $^1H$ -NMR spectrum of compound **4** showed one broad singlet value at  $\delta$  12.42 which revealed chelated hydroxyl groups at C-5 positions. The meta-located protons signal at  $\delta$  6.19 (H-6) and  $\delta$  6.49 (H-8) were observed. The double of a doublet at  $\delta$  7.79 with coupling constants 6.8 Hz and 1.2 Hz could be assigned as H-6'. The doublet at  $\delta$  7.13 with coupling constants 6.8 Hz indicated H-5'. The H-2' displayed the singlet signal at  $\delta$  7.74. The splitting pattern and coupling constants revealed the presence of a trisubstituted benzene ring. The spectrum displayed two singlets at  $\delta$  3.84 and  $\delta$  3.84 indicating the presence of two methoxy groups. The  $^{13}C$ -NMR spectral information of compound **4** contained 17 major signals attributable to five methines, ten quaternaries, and two methyl carbons, which were designated by the HMQC and HMBC spectra of compound **4** along with a comparison with the relevant literature.<sup>22</sup> From this evidence, compound **4** was suggested to be dillenetin (**4**).

Compound **5** was obtained as yellow needles and produced orange color with anisaldehyde-sulphuric acid on TLC with  $R_f$  value 0.42 (30% acetone-hexane). The molecular formula of compound **5** was analyzed as  $C_{15}H_{10}O_7$  by the HR-ESI-TOFMS  $m/z$ : 303.0503  $[M+H]$ . The infrared spectrum presented the presence of hydroxy groups at  $3381\text{ cm}^{-1}$ , conjugated  $\gamma$ -pyrone at  $1660\text{ cm}^{-1}$ , and benzene ring at  $1600\text{ cm}^{-1}$ . The UV absorption maxima in MeOH at 247, 260, 297, 359 and 394 nm were found to belong to a flavonoid skeleton. The  $^1H$ -NMR data of the compound **5** shown two sets of signals. The meta-located protons signal at  $\delta$  6.26 (d,  $J = 0.8\text{ Hz}$ , H-6) and  $\delta$  6.52 (d,  $J = 0.8\text{ Hz}$ , H-8) were observed. Other sets of three protons in an ortho-meta coupled arrangement corresponding to a trisubstituted aromatic ring were also observed at 7.82 (dd,  $J = 6.8, 2\text{ Hz}$ , H-2'), 7.76 (dd,  $J = 6.8, 2\text{ Hz}$ , H-6') and 7.00 (d,  $J = 6.8\text{ Hz}$ , H-5'). The  $^{13}C$ -NMR and the DEPT spectra of compound **5** revealed the presence of 15 aromatic carbon atoms out of which ten are quaternary, and five are olefinic carbon signals. The downfield signal at 175.9 ppm was due to the carbonyl group at C-4. The preceding spectral analysis and similarity with the reported data pointed to the proposed structure of compound **5** as quercetin (**5**).<sup>22</sup>

Compound **6** was obtained as a white amorphous solid with melting point 272-274°C. It gave a purple coloration with anisaldehyde- $H_2SO_4$  reagent as same as that of compound **2**. The  $R_f$  value of compound **6** was found to be 0.45 in 10% MeOH- $CH_2Cl_2$ . On the basis of its HR-ESI-TOFMS ( $[M+Na]^+$  at  $m/z$  599.4288), a molecular formula of compound **6** was established as  $C_{35}H_{60}O_6$ . IR and  $^1H$ -NMR spectral data were used to determine the structure of compound **6**. Its IR was showing the characteristic

peaks at  $3360\text{ cm}^{-1}$  due to the hydroxyl group. The  $^1\text{H}$ -NMR spectrum revealed the peaks of methyl groups at  $\delta$  0.91, 0.80, 0.80, 0.76, 0.70 and 0.68 corresponding to H-18, H-19, H-21, H-29, H-26 and H-27, respectively. The olefinic protons at H-6 showed the signals at  $\delta$  5.37. The anomeric proton (H-1') was observed as doublets at  $\delta$  4.42 ( $J = 7.8\text{ Hz}$ ). The protons corresponding to d-glucose moiety showed the peaks in the range of  $\delta$  4.42-3.43 ppm. Thus, from all the above spectral data, the structure of compound **6** is assigned as  $\beta$ -sitosterol-d-glucoside (**6**).

Table-1:  $^1\text{H}$  (400 MHz) and  $^{13}\text{C}$  (125 MHz) NMR Spectral Data of Kaempferide (**3**), Dillenetin (**4**), and Quercetin (**5**) (**3** in Acetone- $d_6$ ; **4** in DMSO- $d_6$ ; **5** in Acetone- $d_6$ ;  $\delta$  in ppm;  $J$  in Hz.).

Pos.	Kaempferide ( <b>3</b> )		Dillenetin ( <b>4</b> )		Quercetin ( <b>5</b> )	
	$\delta$ $^1\text{H}$ (mult, $J$ (Hz))	$\delta$ $^{13}\text{C}$	$\delta$ $^1\text{H}$ (mult, $J$ (Hz))	$\delta$ $^{13}\text{C}$	$\delta$ $^1\text{H}$ (mult, $J$ (Hz))	$\delta$ $^{13}\text{C}$
2		146.6		146.1		146.9
3		136.9		136.2		136.8
4		177.5		175.9		176.6
4a		104.2		103.0		104.1
5	12.04 (s, 5-OH)	162.1	12.42 (s, 5-OH)	160.7	12.16 (s, 5-OH)	165.0
6	6.27 (d, $J = 1.6\text{ Hz}$ )	99.1	6.19 (d, $J = 1.2\text{ Hz}$ )	98.2	6.26 (d, $J = 0.8\text{ Hz}$ )	99.2
7		165.0		164.0		167.6
8	6.54 (d, $J = 1.6\text{ Hz}$ )	94.0	6.49 (d, $J = 1.2\text{ Hz}$ )	93.6	6.52 (d, $J = 0.8\text{ Hz}$ )	94.5
8a		151.6		156.2		157.8
1'		124.4		123.3		121.5
2'	8.22 (d, $J = 8\text{ Hz}$ )	130.3	7.74 (s)	110.8	7.82 (dd, $J = 2\text{ Hz}$ )	115.7
3'	7.11 (d, $J = 8\text{ Hz}$ )	114.9		148.3		145.8
4'		157.9		146.1		146.9
5'	7.11 (d, $J = 8\text{ Hz}$ )	114.9	7.13 (d, $J = 6.8\text{ Hz}$ )	111.5	7.00 (d, $J = 6.8\text{ Hz}$ )	116.2
6'	8.22 (d, $J = 8\text{ Hz}$ )	130.3	7.79 (dd, $J = 6.8, 1.2\text{ Hz}$ )	121.4	7.69 (dd, $J = 6.8, 2\text{ Hz}$ )	121.52
3'-OCH <sub>3</sub>			3.84 (s)	55.6		
4'-OCH <sub>3</sub>	3.90 (s)	55.8	3.84 (s)	55.6		

### *In vitro* Xanthine Oxidase Inhibitory Activity

The concentration-dependent inhibitory activity of XO was evaluated for all isolated compounds. The XO inhibition resulted in a reduced uric acid production, which was measured spectroscopically at 517 nm, and their inhibitory activities were shown in Table-2. Allopurinol (XO enzyme inhibitor) was used as a reference for positive control in this assay with an  $\text{IC}_{50}$  value of  $0.12 \pm 0.01\text{ mM}$ . Among the isolated compounds, quercetin was found to possess the highest activity ( $\text{IC}_{50}$   $0.56 \pm 0.11\text{ mM}$ ). The activity of quercetin was found to be 4-folds lower than the standard, allopurinol. Kaempferide and dillenetin showed lesser activity with an  $\text{IC}_{50}$  value of  $1.44 \pm 0.04$  and  $0.76 \pm 0.17\text{ mM}$ , respectively. Whereas all other isolated compounds were inactive (inactive at  $600\text{ }\mu\text{g/mL}$ ). Our findings are consistent with previous reports, which indicated that flavonols were xanthine oxidase inhibitors.<sup>31,32</sup> Regarding XO inhibitory activity, all obtained flavonols were decided on further *in silico* molecular docking studies.

Table-2: XO Inhibitory Activities of Compounds **1-6**.

Compound	$\text{IC}_{50}^a \pm \text{SD (mM)}$
Lupeol ( <b>1</b> )	Inactive <sup>b</sup>
A mixture $\beta$ -sitosterol and stigmasterol ( <b>2</b> )	Inactive <sup>b</sup>
Kaempferide ( <b>3</b> )	$1.44 \pm 0.04$
Dillenetin ( <b>4</b> )	$0.56 \pm 0.11$
Quercetin ( <b>5</b> )	$0.76 \pm 0.17$
$\beta$ -Sitosterol-d-glucoside ( <b>6</b> )	Inactive <sup>b</sup>
Allopurinol <sup>c</sup>	$0.12 \pm 0.01$

<sup>a</sup>Results are displayed as means of  $\text{IC}_{50}$  values in mM, and the data were retrieved from triplicate tested.

<sup>b</sup>Inactive at  $600\text{ }\mu\text{g/mL}$  (highest concentration tested).

<sup>c</sup>Standard used for the assay.

### *In silico* Docking Studies

The binding interaction among the chosen compounds and XO enzyme (1FIQ) was analyzed by *in silico* molecular docking studies. A docking experiment was carried out using AutoDock docking software to explain the mode of interaction between the binding sites of the XO enzyme and the isolated phenolic compounds. In order to verify the efficacy of the applied docking parameters, the cocrystallized ligand salicylic acid was redocked toward the active site of XO, and the root-mean-square deviation (RMSD) was 0.88 Å guaranteed the validity of the docking procedure.

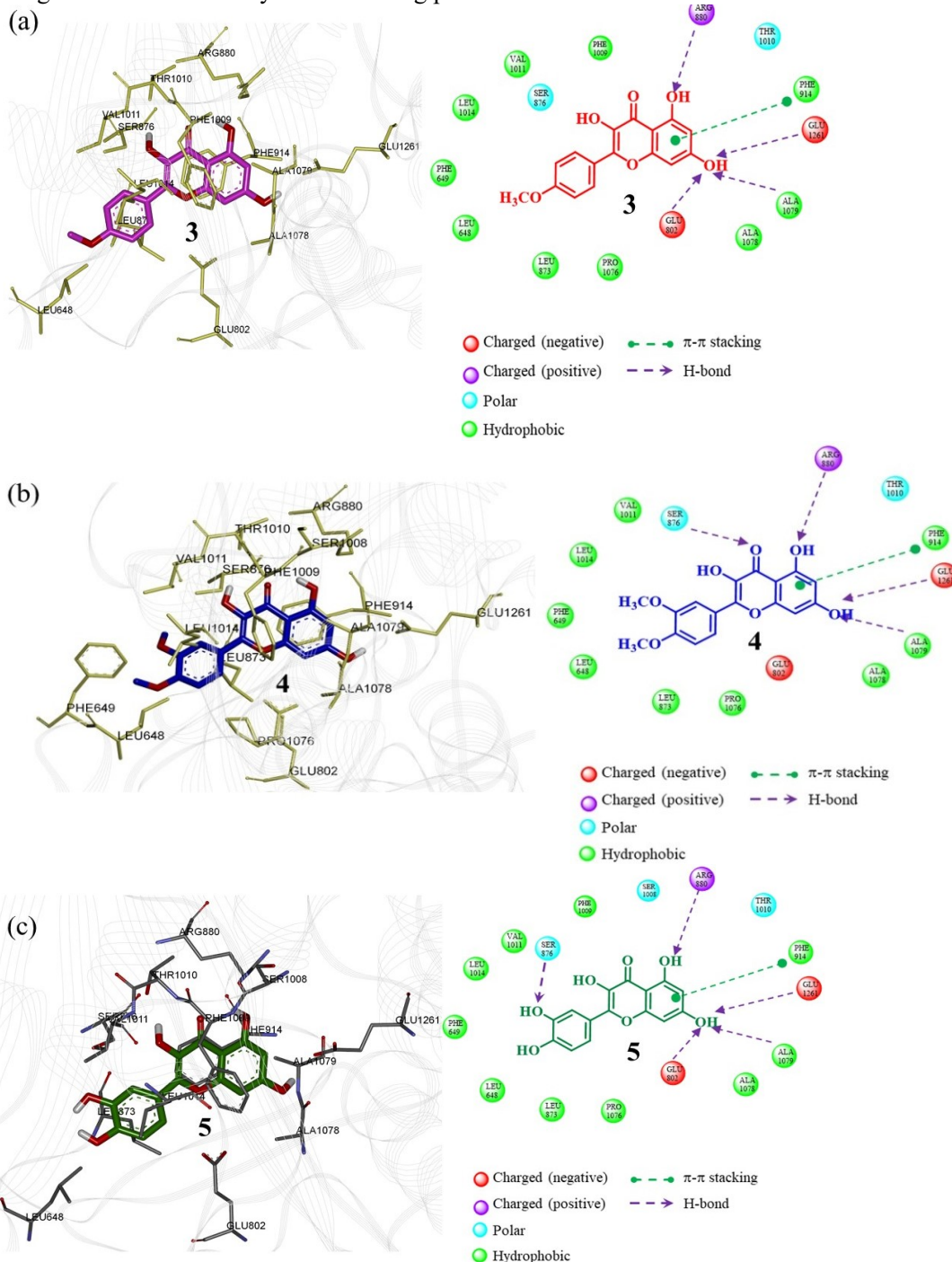


Fig.-2: The 2D and 3D Interaction Poses of the Selected Molecule in the Active Pocket of 1FIQ. ((A) Kaempferide (3), (B) Dillenetin (4) and (C) Quercetin (5))



All the isolated flavonols were used to dock studies with the 1FIQ. The results of molecular docking were summarized in Table-3. The picture of 2D and 3D docking results of the best conformer were manifested in Fig.-2. Based on the interaction of AutoDock, the result was analyzed. All three isolated flavonols (**3**, **4** and **5**) showed a similar mode of interactions. The molecular docking investigation confirmed that **3**, **4** and **5** were substantially positioned within the salicylic acid XO enzyme's active site. The minimum binding energies of **3**, **4** and **5** were -11.38, -10.54 and -11.59 kcal mol<sup>-1</sup>, respectively. These results are consistent with the results obtained on *in vitro* XO inhibition assays. All compounds were enclosed by particular amino acids (Glu802, Arg880 and Glu1261), which were defined as catalytic residues of XO.<sup>33</sup> The best-rankings docked structure of the most potent compound **5** clarified that the compound possesses six hydrogen bonds and one  $\pi$ - $\pi$  interactions with the active site. The hydroxyl groups connected to the A ring of the compound created hydrogen bonds interaction, including Glu802, Arg880, Ala1079 and Glu1261. One hydrogen bond among the ring B hydroxyl groups of the compound and Ser876 was similarly inspected. Moreover, a  $\pi$ - $\pi$  interactions connecting the compound and the active site residues (Phe914) was also discovered. The greatest activity of compound **5** may be due to the occurrence of hydroxyl groups connected to ring B. Both the hydroxyl groups are involved in bonding. The presence of hydroxyl groups makes the molecule more polar and promote compound **5** to make particular interactions with XO active site.

Five hydrogen bonds and two  $\pi$ - $\pi$  interactions with crucial active site residues were observed in the second most active compound (Dillinenetin (**4**)) in the sequence. Ser876 interacted with the methoxy group of the compound. Compound **4**, however, was significantly less active than compound **5**, due to the lack of contact between the hydroxyl groups at ring B and the active residue site.

In the case of kaempferide (**3**), five hydrogen bonds were observed with the important residues of the active site. Phe914 was found in  $\pi$ - $\pi$  interaction with A ring moiety of the compound **3**. However, kaempferide (**3**) displayed lower activity than quercetin (**5**) due to the absence of the C-3' hydroxyl group.

Table-3: Molecular Docking Experiments: Binding of Interactions of the Selected Compounds with XO (1FIQ)

Residual	Kaempferide ( <b>3</b> )		Dillinenetin ( <b>4</b> )		Quercetin ( <b>5</b> )	
	Type of interaction (Amino-ligand)	Distance (Å)	Type of interaction (Amino-ligand)	Distance (Å)	Type of interaction (Amino-ligand)	Distance (Å)
LEU648	C-O	3.487	C-O	3.507	C-O	3.545
PHE649	-	-	C-C	3.883	-	-
GLU802	O-H-bond	3.375	$\pi$ - $\pi$	3.255	O-H-bond	3.473
LEU873	C-C	3.362	C-C	3.264	C-C	3.477
SER876	C-O	3.892	O-C	3.151	O-H-bond	3.331
ARG880	N-H-bond	2.627	N-H-bond	2.884	N-H-bond	2.631
PHE914	$\pi$ - $\pi$	3.425	$\pi$ - $\pi$	3.562	$\pi$ - $\pi$	3.644
SER1008	C-C	3.522	-	-	O-O interaction	3.981
PHE1009	-	-	-	-	C-C	3.988
THR1010	O-H-bond	3.035	N-H-bond	2.800	N-H-bond	3.043
VAL1011	N-H-bond	3.364	C-O	3.074	C-O	3.208
LEU1014	C-C	3.513	C-C	3.179	C-C	3.304
PRO1076	-	-	C-C	3.905	-	-
ALA1078	C-C	3.782	C-C	3.568	C-C	3.689
ALA1079	N-H-bond	3.189	N-H-bond	3.087	N-H-bond	3.137
GLU1261	O-H-bond	2.989	O-H-bond	3.203	O-H-bond	2.784

## CONCLUSION

In conclusion, *D. Indica* fruits are a good source of the anti-XO agent to treat gout and related disorders. The XO properties of *Dillenia* species are due to the presence of flavonols as a constituent. Three isolated

flavonols, **3**, **4** and **5**, with IC<sub>50</sub> values of 1.44 ± 0.04 mM, 0.56 ± 0.11 mM and 0.76 ± 0.17 mM, respectively, showed good XO inhibitory activity almost identical to allopurinol standard drug. (IC<sub>50</sub>, 0.12 ± 0.01 mM). In addition, the molecular modeling study of the potent compound **3**, **4** and **5** indicated that XO accommodated them, nicely. In order to develop potential chemical entities for clinical use in the prevention and treatment of gout, further investigations on the above compounds and *in vivo* studies are necessary.

### ACKNOWLEDGMENT

This work was financed by a grant from Phranakhon Rajabhat University in Thailand. The authors are grateful to the Faculty of Science and Technology, Phranakhon Rajabhat University, for providing all the necessary facilities in the laboratory. Grateful acknowledgment is made to the Department of Chemistry, Faculty of Science, Srinakharinwirot University, Thailand for providing necessary infrastructure facilities for the docking study.

### REFERENCES

1. T. Bardin and P. Richette, *BMC Medicine*, **15**, 123 (2017), DOI:10.1186/s12916-017-0890-9
2. E. Roddy and M. Doherty, *Arthritis Research & Therap*, **12**(6), 223(2010), DOI: 10.1186/ar3199.
3. A. Finch and P. Kubler, *Australian Prescriber*, **39**(4), 119(2016), DOI:10.18773/austprescr.2016.047
4. G. Calogiuri, E. Nettis, E. Di Leo, C. Foti, A. Ferrannini and L. Butani, *Inflammation & Allergy - Drug Targets*, **12**(1), 19(2013), DOI:10.2174/1871528111312010004
5. C.C. Hung, W.C. Liu, M.C. Kuo, C.H. Lee, S.J. Hwang and H.C. Chen, *American Journal of Nephrology*, **29**(6), 633(2009), DOI:10.1159/000195632
6. C. Katiyar, A. Gupta, S. Kanjilal and S. Katiyar, *Ayu*, **33**(1), 10(2012), DOI:10.4103/0974-8520.100295
7. S. Jyothi, Y.V. Subba Rao and P.S. Samuel Ratnakumar, *RASĀYAN Journal of Chemistry*, **12**(2), 537(2019), DOI: 10.31788/RJC.2019.1225000
8. S. Fatema, M. Farooqui, M. Ubale and P. M. Arif, *RASĀYAN Journal of Chemistry*, **12**(2), 616 (2019), DOI:10.31788/RJC.2019.1222065
9. J.A.O. Olugbuyiro, A.S. Banwo, A.O. Adeyemi, O.S. Taiwo and O. A. Akintokun, *RASĀYAN Journal of Chemistry*, **11**(2), 798 (2018), DOI:10.31788/RJC.2018.1121823
10. M.M. Hudaib, K.A. Tawaha, M.K. Mohammad, A.M. Assaf, A.Y. Issa and F.Q. Alali, *Pharmacognosy Magazine*, **7**(28), 320(2011), DOI:10.4103/0973-1296.90413
11. T. Smitinand, 2001, Thai plant names, Office of the Forest Herbarium, Department of National Park, Wildlife and Plant Conservation, National Office of Buddhism Press, Bangkok, pp. 201-202.
12. M.N. Parvin, M.S. Rahman, M.S. Islam and M.A. Rashid, *Bangladesh Journal of Pharmacology*, **4**, 122(2009), DOI:10.3329/bjp.v4i2.2758
13. M.H. Abdille, R.P. Singh, G.K. Jayaprakash and B.S. Jena, *Food Chemistry*, **90**(4), 891(2005), DOI:10.1016/j.foodchem.2004.09.002
14. P.A. Singh, N.B. Brindavanam, G.P. Kimothi and V. Aeri, *Asian Pacific Journal of Tropical Disease*, **6**(1), 75(2016), DOI:10.1016/S2222-1808(15)60988-4
15. M.M. Fatema, H. Mofazzal, H. Mehedi and R.R. Satyajit, *International Journal of Pharmaceutical Sciences and Research*, **7**(1), 136(2016), DOI:10.13040/IJPSR.0975-8232.7(1).136-43
16. A.T.M. Silva, C.G. Magalhães, L.P. Duarte, W.N. Mussel, A.L.T.G. Ruiz and L. Shiozawa, *Brazilian Journal of Pharmaceutical Sciences*, **53**(3), 1(2017), DOI:10.1590/s2175-97902017000300251
17. C.K. Lee, P.H. Lee and Y.H. Kuo, *Journal of the Chinese Chemical Society*, **48**(6A), 1053(2001), DOI:10.1002/jccs.200100154
18. M.E. Haque, M.N. Islam, D.D. Gupta, M. Hossain, H.U. Shekhar and B.A. Shibib, *Dhaka University Journal of Pharmaceutical Sciences*, **7**(1), 4(2008), DOI:10.3329/dujps.v7i1.1221
19. I.S. Okoro, T.A. Tor-Anyiin, J.O. Igoli, X.S. Noundou and R.W.M. Krause, *Asian Journal of Chemical Sciences*, **3**(4), 1(2018), DOI:10.9734/AJOCS/2017/37147
20. A.P. Rajput and T.A. Rajput, *International Journal of Biological Chemistry*, **6**(4), 130(2012), DOI:10.3923/ijbc.2012.130.135

21. V.S. Nguyen, L. Shi, F.Q. Luan and Q.A. Wang, *Acta Biochimica Polonica*, **62(3)**, 547(2015), DOI:10.18388/abp.2015\_992
22. D.T.D. DeSilva, D.M.S. Bahorun and D.L.M. Huong, 2009, *Traditional and Alternative Medicine: Research and Policy Perspectives*, Daya Publishing House, Delhi, pp. 612.
23. M. Khatun, M. Billah and M.A. Quader, *Dhaka University Journal of Science*, **60(1)**, 6(2012), DOI:10.3329/dujs.v60i1.10327
24. V.S.P. Chaturvedula and I. Prakash, *International Current Pharmaceutical Journal*, **1(9)**, 4(2012), DOI:10.3329/icpj.v1i9.11613
25. Y. Niu, H. Zhu, J. Liu, H. Fan, L. Sun and W. Lu, *Chemico-biological interactions*, **189(3)**, 161(2011), DOI:10.1016/j.cbi.2010.12.004
26. C. Enroth, B.T. Eger, K. Okamoto, T. Nishino, T. Nishino and E.F. Pai, *Proceedings of the National Academy of Sciences*, **97(20)**, 10723(2000), DOI:10.1073/pnas.97.20.10723
27. G.M. Morris, R. Huey, W. Lindstrom, M.F. Sanner, R.K. Belew and D.S. Goodsell, *Journal of Computational Chemistry*, **30(16)**, 2785(2009), DOI:10.1002/jcc.21256
28. ACD/Structure Elucidator, version 2018.1, 2019, Advanced Chemistry Development, Inc., Toronto.
29. M.J. Frisch, G.W. Trucks, H.B. Schlegel, G.E. Scuseria, M.A. Robb and J.R. Cheeseman, 2004, Gaussian 03, Gaussian, Inc., Connecticut.
30. M. Kontoyianni, L.M. McClellan and G.S. Sokol, *Journal of Medicinal Chemistry*, **47(3)**, 558(2004), DOI:10.1021/jm0302997
31. P. Cos, L. Ying, M. Calomme, J.P. Hu, K. Cimanga and B. Van Poel, *Journal of natural products*, **61(1)**, 71(1998), DOI:10.1021/np970237h
32. D. Di Majo, M. La Guardia, G. Leto, M. Crescimanno, C. Flandina and M. Giammanco, *International Journal of Food Sciences and Nutrition*, **65(7)**, 886(2014), DOI:10.3109/09637486.2014.931362
33. H. Cao, J.M. Paufl and R. Hille, *Journal of Biological Chemistry*, **285(36)**, 28044(2010), DOI:10.1074/jbc.M110.128561

[RJC-5412/2019]